*Desalination and Water Treatment*
www.deswater.com
doi: 10.5004/dwt.2022.28975

280 (2022) 197–205
December

# Treatment of glyphosate by-product phosphorus-containing waste salt by a combined ultrafiltration and nanofiltration process

Qisheng Wu*, Weijian Zhang, Ming Jiang

*College of Materials Science and Engineering, Yancheng Institute of Technology, Yancheng, 224051, China, emails: qishengwu@ycit.cn (Q. Wu), 835584559@qq.com (W. Zhang), 1779965378@qq.com (M. Jiang)*

Received 2 May 2022; Accepted 5 October 2022

**ABSTRACT**

The feasibility of treating glyphosate by-product phosphorus-containing waste salt by hybrid ultrafiltration–nanofiltration is investigated. The ultrafiltration removal and permeability were tested to select a suitable upstream membrane module. On this basis, the effects of subsequent conditions on the nanofiltration fraction of the combined process, such as permeate concentration, pH, and pressure applied to the nanofiltration, on membrane removal of total phosphorus and chloride ions. The optimal conditions were used to remove total phosphorus and retain sodium chloride. Scanning electron microscopy analysis was also performed on the nanofiltration, and the fouling was within the membrane surface pores. Results show that the upstream use of ultrafiltration can better remove impurities and relieve the pressure of nanofiltration. In the nanofiltration part, the maximum total phosphorus removal rate of 96.28% and the minimum chloride removal rate of 46.38% can be achieved when the permeate concentration is 330 g/L, pH = 10.0 and pressure is 2.6 MPa, and the membrane flux can reach 210 L/m$^2$·h when the above results are maintained. Molecular weight cut-off of 5,000 and 150 Da for the two membranes, respectively.

*Keywords:* Glyphosate; Waste salt; Ultrafiltration; Nanofiltration; Phosphorus removal rate

## 1. Introduction

Glyphosate has only been on the market since the mid-1970s. It is considered by many analysts and most governments to be a relatively safe herbicide compared to other more toxic chemical herbicides. Still, there is growing public concern about the consequences of its increased use in agriculture [1]. As a widely used herbicide in the world, its main production methods are the iminodiacetic acid method (IDA) [2] and the alkyl ester method (alkyl phosphite method, glycine method) [3].

In production using the glycine method, for every 1 t of glyphosate produced, 5–6 t of crystalline mother liquor will be produced, which contains about 1% glyphosate, 1%–4% formaldehyde, and a large number of by-products [4]. A large amount of triethylamine in the by-product is usually recovered by adding NaOH. Still, it also increases the NaCl content in the crystallization of mother liquor, which raises the difficulty of the mother liquor recovery [5,6]. Why glyphosate by-product waste salt obtained by evaporation and crystallization cannot be directly used is that it contains a large amount of TP (Total of phosphorus that exists in the wastewater in both inorganic and organic forms) and TOC (Total amount of dissolved and suspended organic matter containing carbon in wastewater), of which the TP content can be more than 2,000 mg/kg. Recently, the methods used to remove phosphorus are usually electrochemical techniques, chemical precipitation, biological treatment, and membrane separation [7–10]. Membrane separation is widely used for phosphorus removal mainly due to its simple operation, stable operation, higher selectivity of phosphorus, less waste generated, and efficient removal of phosphorus by simply

* Corresponding author.

setting up the operation method and initial conditions of the separated solution [11,12].

In membrane separation processes, ultrafiltration that retains larger molecular weights is exhibited to keep phosphate, and small molecules pass through ultrafiltration as permeate when mixed solutions of large and small molecules pass through ultrafiltration [13]. Moreover, nanofiltration showed high retention of phosphate and great potential in phosphorus recovery [14,15]. Nanofiltration as a separation membrane can withstand a wide pH range, retain molecular weights between 100–1,000 Da, have pore sizes between 0.5–2 nm, have significant selective permeability for small and large molecules, and have a retention capacity between ultrafiltration and reverse osmosis [16–18]. It is mainly used to separate inorganic salts [19], antibiotics [20], heavy metals [21], dyes [22], pigments [23], and other multivalent ions or small organic molecules. The selective permeability of nanofiltration membranes is also demonstrated by their negatively charged surface, which allows more effective removal of higher valence ions, especially in removing divalent ions [24–26]. Bargeman et al. [27] have done extensive experiments and even found that nanofiltration has a negative retention effect on monovalent salts, especially chlorides, which is highly beneficial to our study and retention of the desired NaCl. In recent years, many phosphorus recovery studies have tested ultrafiltration and nanofiltration, respectively. Ultrafiltration's total phosphorus recovery capacity is less than 50%, while nanofiltration is higher than 90% [28–30]. Since ultrafiltration has a higher molecular weight cut-off (MWCO) [31] than nanofiltration, nanofiltration is more prone to fouling in the process of phosphorus recovery, which significantly affects the long-term use of nanofiltration and increases the cost of using nanofiltration separation [17,32].

Therefore, using only one ultrafiltration or nanofiltration cannot achieve our goal of recovering phosphorus and retaining NaCl; the phosphorus was recovered using the dual membrane process (DMP) [33]. Upstream ultrafiltration is set up to mitigate pollution, and downstream nanofiltration is mainly responsible for recovering phosphorus. Current methods focus on ultrafiltration–nanofiltration (UF-NF) hybrid separation to remove phosphorus in brackish water to 0.5 g/L [33,34]. This hybrid process achieved a removal rate of less than 40% for chlorine, which indicates the feasibility of mixing the two separation membranes [35].

This study evaluated the performance of a hybrid UF-NF process in removing TP from a high salt waste salt to obtain higher TP removal and lower NaCl removal. To maximize the TP removal, tests were carried out with a focus on NF, focusing on concentration, pH, pressure, and NF pore size in terms of reduction. The fouling of the NF surface after long-term use was also investigated. The aim is to provide new insights into the field of waste salts with the high phosphorus content.

## 2. Experimental part

### 2.1. Industrial high salinity waste salt

The industrial waste salt is used by the ultrafiltration–nanofiltration system, which is glyphosate by-product waste salt derived from Hubei Xingfa Chemical Group Co., Ltd., China, calcined at a high temperature of 550°C [36]. The major components of the waste salt are shown in Table 1:

### 2.2. Membranes and experimental equipment setup

Hydrochloric acid and sodium hydroxide were analytically pure reagents used to adjust the pH. The rolled hollow fiber membrane and the secondary membrane separation tester were provided for experiments (DMJ60-2, Bona, Shandong, China). Nanofiltration membrane module, separation equipment, and testing equipment used for separation, permeability, and selectivity were washed with distilled water and dried separately. The main characteristics of the membrane module used in the experiment as in Table 2.

Used for laboratory-scale ultrafiltration–nanofiltration separation equipment, secondary membrane separation testing machine flow chart as shown in Fig. 1. Mainly raw material pot, circulating water pump, membrane module,

Table 1
Significant parts of the waste salt

| Characteristics | Waste salt |
|---|---|
| pH | 10.05 |
| TP, mg/kg | 2,923 |
| NaCl, % | 98 |
| $Ca^{2+}$, mg/kg | 34 |
| $Mg^{2+}$, mg/kg | 26 |
| $Ba^{2+}$, mg/kg | 0.04 |
| $Fe^{2+}$, mg/kg | 3 |

Table 2
Specifications of the membrane module

| Membrane | Theoretical MWCO | pH | Temperature tolerance (°C) | Max. operating pressure (MPa) | Area ($m^2$) |
|---|---|---|---|---|---|
| NF-100Da | 100 Da | 2–12 | 5–55 | 3.8 | 0.042 |
| NF-150Da | 150 Da | 2–12 | 5–55 | 3.8 | 0.042 |
| NF-300Da | 300 Da | 2–12 | 5–55 | 3.8 | 0.042 |
| NF-600Da | 600 Da | 2–12 | 5–55 | 3.8 | 0.042 |
| UF-1000Da | 1,000 Da | 2–12 | 5–55 | 0.5 | 0.049 |
| UF-5000Da | 5,000 Da | 2–12 | 5–55 | 0.5 | 0.049 |

MWCO: The minimum molecular weight cut-off at which the separating membrane can retain 90% of the solute is the MWCO [31].

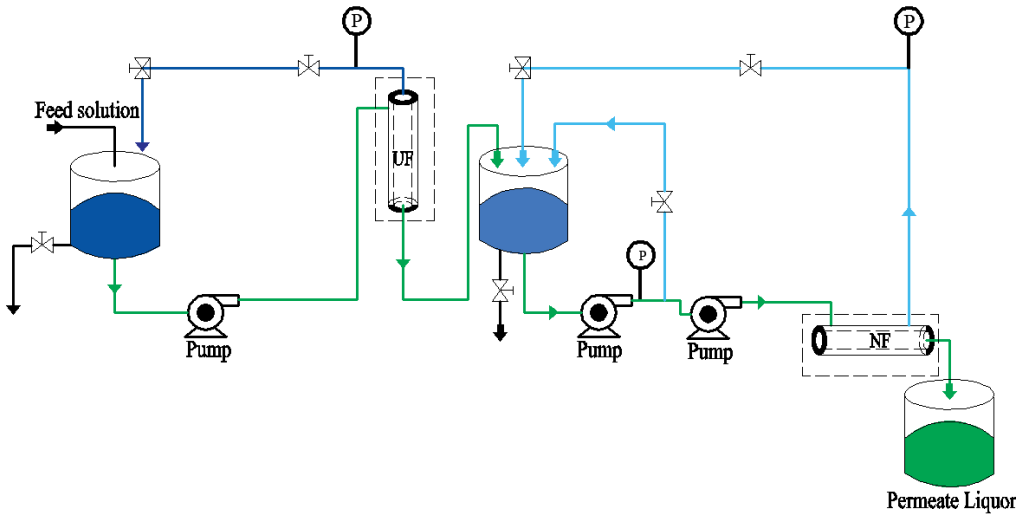


Fig. 1. Ultrafiltration–nanofiltration membrane separation equipment.

pressure gauge, flow meter, regulator, discharge valve, and other components. The raw material pot was transported to the first level of ultrafiltration through the circulating water pump. Under the pressure drive, the suspended impurities and insoluble materials are retained by ultrafiltration, and the clarified filtrate enters the nanofiltration separation part. After entering the secondary membrane separation system was driven by high pressure, and the clarified filtrate with high NaCl and low TP content was obtained. The remaining filtrate is sent for further processing.

The total phosphorus content in the solution was determined using a total phosphorus rapid tester (SH-50TN, Sheng'aohua, Jiangsu, China), pH-meter (PHS3-C) supplied by Shanghai Yidian Scientific Instruments Co., China.

### 2.3. Data processing

In the separation process, the following equations are used to represent the removal of total phosphorus as well as chloride ions [37]:

$$R = \left(1 - \frac{C_p}{C_f}\right) \times 100\% \tag{1}$$

where $C_p$ and $C_f$ are the permeate and feed concentrations, respectively.

The flux ($J_v$) is the volume of the permeate ($V_p$) collected per unit membrane area ($A$) per unit time ($t$):

$$J_v = \frac{V_p}{A \times t} \tag{2}$$

The concentration of $C_R$ removed by the membrane is expressed by the following mass balance equation:

$$C_R V_R = C_0 V_0 - C_p V_p \tag{3}$$

where $C_0$ and $V_0$ is concentration and volume in the feed, $V_R = V_0 - V_p$.

The total phosphorus removal (%) is represented as:

$$R_{TP} = \frac{C_{R,TP}}{C_{0,TP}} \times 100\% \tag{4}$$

The $Cl^-$ removal (%) is represented as:

$$R_{Cl^-} = \frac{C_{R,Cl^-}}{C_{0,Cl^-}} \times 100\% \tag{5}$$

The total phosphorus permeate (%) is represented as:

$$P_{TP} = \frac{C_{P,TP}}{C_{0,TP}} \times 100\% \tag{6}$$

The $Cl^-$ permeate (%) is represented as:

$$P_{Cl^-} = \frac{C_{P,Cl^-}}{C_{0,Cl^-}} \times 100\% \tag{7}$$

## 3. Results and discussion

To prevent each group of tests from interfering, interval washing was utilized to clean the secondary membrane separation equipment and an additional buffer tank between UF and NF to recover primary permeate.

### 3.1. Selection of UF membrane

Experiments were performed in the first part of a hybrid ultrafiltration–nanofiltration system, using ultrafiltration to evaluate their selectivity for phosphorus and chlorine and select the appropriate membrane upstream. For the above problems, two membranes were used to conduct

the experiments. Given a pressure of 0.4 MPa, the effective area of ultrafiltration was 0.049 $m^2$, while the pure water fluxes of UF-5000Da and UF-1000Da were (768 $L/m^2 \cdot h$) and (558 $L/m^2 \cdot h$). As shown in Fig. 2, both UF-5000Da and UF-1000Da can remove insoluble and suspended impurities to relieve the subsequent NF membrane pressure, UF-1000 removed sodium chloride higher and provided lower sodium chloride for subsequent separations, and increased the possibility of membrane surface fouling. The UF-5000Da was selected as the upstream in all following cases, which is beneficial to obtain more sodium chloride.

### 3.2. Selection of NF membrane

#### 3.2.1. Effect of waste salt concentration

The pH of the feed solution was controlled to be 10, the operating pressure of ultrafiltration was 0.4 MPa, and the nanofiltration with MWCO of 100, 150, 300, and 600 were selected for experiments, and the working pressure was 2.4 MPa. Combined ultrafiltration–nanofiltration separation was conducted for different concentrations of glyphosate by-product salt solution. The total phosphorus and NaCl removal rate were measured, as shown in Fig. 3.

Variations in concentration lead to the production of permeates with different removal rates. The slow increase in concentration reflects the increased removal of TP and chloride ions. Owing to the phenomenon of concentration polarization, the concentration of the solution on both sides of the NF is changed, resulting in the actual concentration difference on the two edges of the membrane being lower than the concentration difference between the feed solution and the permeate. Moreover, as the concentration increases, more charged ions cannot pass through the nanofiltration membrane, producing the Gibbs–Donnan effect [38,39]. This results in the actual osmotic pressure difference being lower than the theoretical osmotic pressure difference, and the TP and NaCl content on the surface of the nanofiltration membrane increases significantly. The liquid concentration becomes an essential research factor. However, although the concentration trend increased, the nanofiltration membranes with different MWCO showed different conditions. As shown in Fig. 3, 100 and 150 Da with low MWCO showed high removal of TP, reaching 96.28% and 96.79% at a concentration of 330 g/L, reaching 96.73% and 96.62% at a concentration of 350 g/L, respectively. The low molecular weight cut-off in the chloride removal diagram also showed a high chloride removal rate. Still, it reached a relatively low chloride removal rate of 46.38% and 47.71% at 300 g/L, 46.92%, and 47.96% at 350g /L, respectively. The larger pore size nanofiltration used in the test had no significant benefit in the two measured removal rates; larger MWCO due to 300 and 600 Da resulted in lower removal rates for TP and chlorides. But an only relative of TP and chloride ions due to their conditions, and no significant advantage compared to 150 and 100 Da, considering that the three-stage membrane system may be placed in the middle to reduce the removal pressure of the next membrane stage. The high concentration of the initial stream can also cause scaling on the surface of the nanofiltration, which is detrimental to its long-term use. NF is much more effective in removing sizeable molecular weight TP than chloride ions in Fig. 3. In conclusion, a concentration of 330g/L was selected as the optimized concentration for secondary membrane separation with lower chloride removal and TP removal.

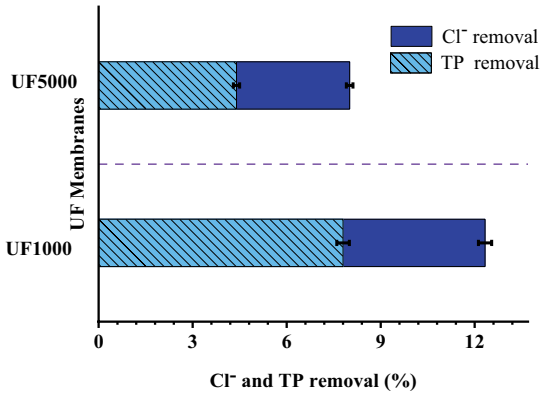


Fig. 2. Removal of a UF membrane.

#### 3.2.2. Effect of waste salt initial pH

From the above experimental results, the retention of acidity and alkalinity in the nanofiltration process was

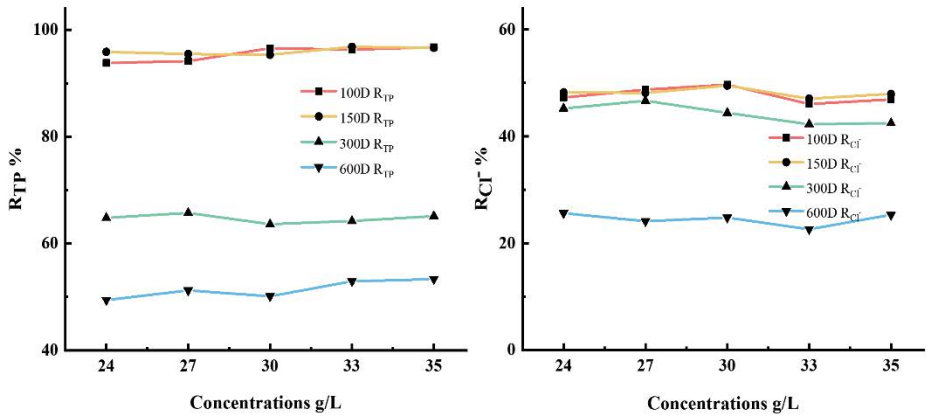


Fig. 3. Effect of waste salt concentration.

analyzed; therefore, an initial concentration of 330 g/L was selected for subsequent experiments. The pressure and the way of washing between each experiment were consistent with what was done before. Selecting the suitable pH is the critical condition for the successful separation of this secondary membrane process, and it was found that different pH levels have a significant influence on it through experiments.

By observing Fig. 4, pH considerably affects the removal rate, with a lower TP removal rate under acidic conditions. In contrast, the effect under alkaline conditions significantly improved compared to it. Optimal concentration removal rates for the above steps were tested with acid, neutral and alkaline, respectively. The specific alkaline value was tested after the initial analysis of the high alkaline removal rate. Cross-sectional observation of Fig. 4, all MWCO of nanofiltration in alkaline conditions total phosphorus removal rate is higher than acidic 10%–20%, which is analyzed because the desalination of monovalent anion salt solution by nanofiltration is lower than that of high-valent anion salt solution, and the ionization degree of $H_3PO_4$, $H_2PO_4^-$ and $HPO_4^{2-}$ increases with the increase of pH, that is, the phosphate in solution mainly existed in the form of phosphate divalent ions, which is beneficial to its removal by nanofiltration. Lower pH increases the concentration of hydrogen ions collected on the membrane surface, forming an electrical double layer, which is also responsible for easier phosphate permeation through nanofiltration [40,41]. The molecular weight retained by the NF membrane itself remains an essential factor in the longitudinal analysis of Fig. 4. At alkaline pH = 10, the 100 Da NF achieved a maximum removal rate of 98.86% for total phosphorus, which was the maximum among all experiments, but also increased the loss of chloride ions by an average of 10% more than the 150 Da NF. In comparison, the 150 Da NF selected achieved a removal rate of 98.52% for total phosphorus and a relatively low removal rate of 47.3% for chloride ions under these conditions.

### 3.2.3. Effect of nanofiltration pressure

To evaluate the feasibility of nanofiltration pressure in removing total phosphorus and chloride ions, $C_p$ and $V_p$ were measured at different pressures for the four pore-size nanofiltration membranes used.

As the pressure decreases, the osmotic pressure of the waste salt solution decreases, and the NF membrane mass transfer capacity decreases, resulting in a reduction in the concentration polarization and a thinning of the boundary layer on the membrane surface where the solution collects [42].

As shown in Fig. 5, the experimental results that are match to the mathematical model (6) made by Ming Xie et al. [43], the 100 Da nanofiltration membrane removed 96% of the total phosphorus. It removed 56% of the chloride ions when the ratio of the permeate volume to the feed liquid volume reached 1. Pressure-driven nanofiltration process can be simulated in a simplified way based on the removal equation with the mass balance equation. The solute loss in the feed solution is equal to the solute loss in the permeate in a constant volume system:

$$V_0 dC = -C dV_p \tag{8}$$

$$-V_0 \ln C_P = V_p + C_x \tag{9}$$

At $V_p = 0$ and $C = C_0$, assuming that the removal is constant, the following equation can be obtained:

$$-V_0 \ln C_P = V_p + V_0 \ln C_0 \tag{10}$$

$$\frac{C_p}{C_0} = \exp\left(-\frac{V_p}{V_0}\right) \tag{11}$$

The results calculated from Eq. (9) are shown in Fig. 5. Fitting the data as well as taking logarithms of the horizontal and vertical coordinates, it was found that the data fit results in a horizontal line. And the result obtained from Eq. (9) should be a positive proportional function after the mentioned treatment, which further indicates that the pressure has almost no effect on the removal of TP and Cl. As seen in Fig. 5b, the membrane with an MWCO of

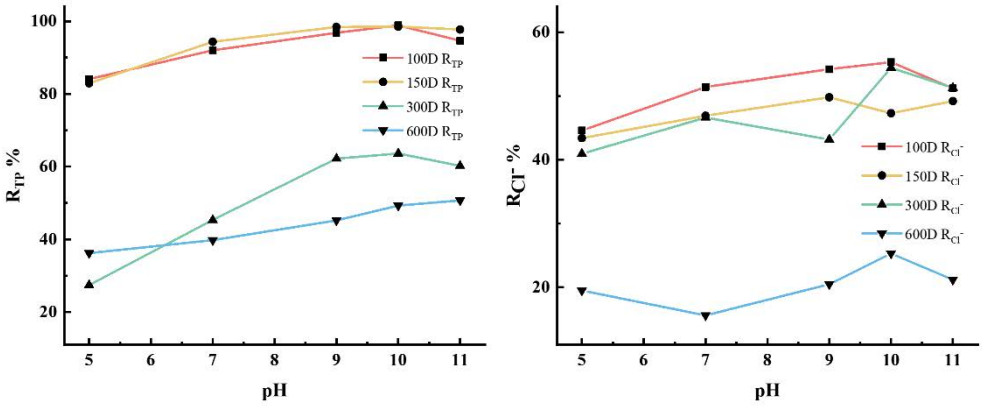


Fig. 4. Effect of waste salt initial pH.

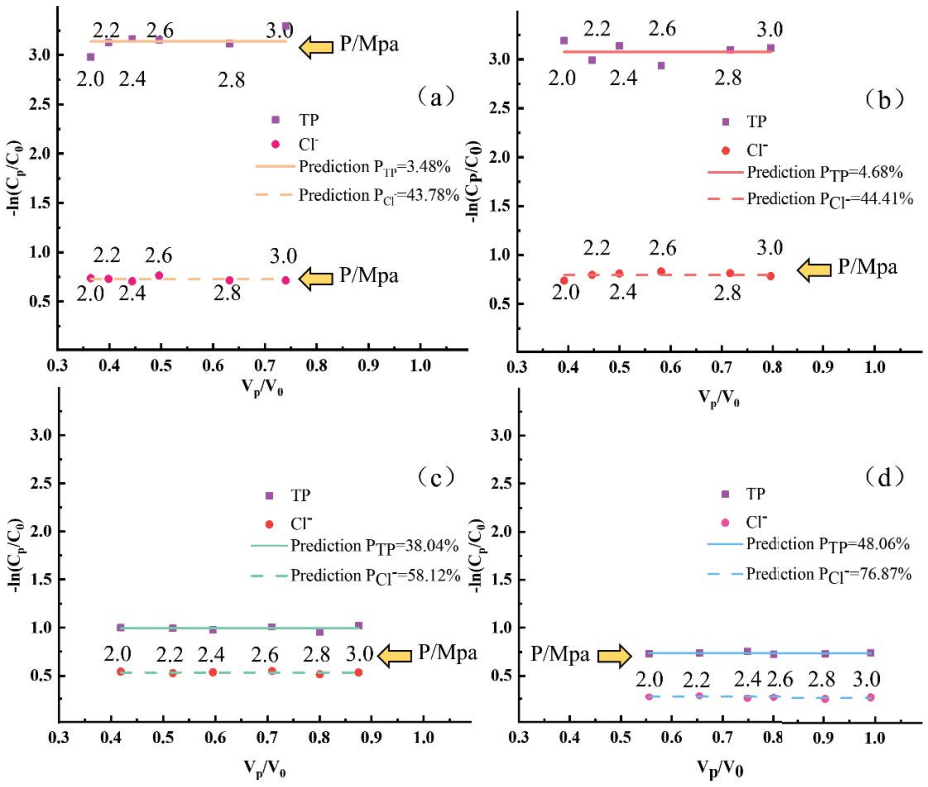


Fig. 5. Results of membrane experiments and simulation: (a) 100 Da, (b) 150 Da, (c) 300 Da, and (d) 600 Da.

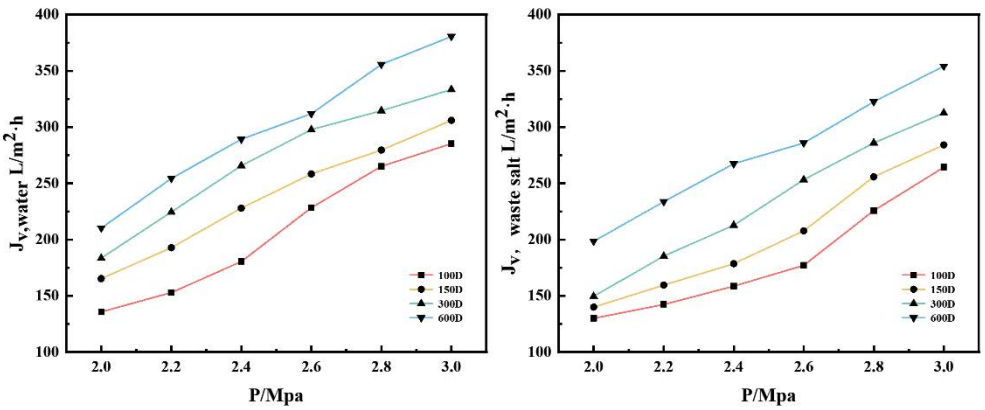


Fig. 6. Permeability of pure water and waste salt solution.

150 Da at 2.6 MPa showed a slightly lower TP permeate than the predicted removal, using 2.6 MPa as the nanofiltration pressure, based on the previously selected concentration and pH.

The effect of pressure on the membrane is also reflected in the change of membrane flux. When the pressure applied to the membrane surface increases, the membrane flux of pure water and the waste salt solution becomes higher, and the experimental results are shown in Fig. 6.

### 3.2.4. Membrane fouling

Nanofiltration fouling varies with pressure, salt concentration, temperature, and other conditions. Fouling quickly but behaves in a complex way [44]. The fouling process also includes membrane material, porosity, operating conditions, permeate quality, membrane surface roughness, membrane surface physical and chemical properties, etc. [45]. The following displays the morphological observation of the contaminated 100 Da nanofiltration membrane surface using field emission scanning electron microscopy (SEM). The thickness of the plating layer was controlled to be 2–8 nm to reflect the actual surface morphology of the used nanofiltration membrane. Due to the limited SEM observation magnification, the coating pores on the surface of the observed membrane were blocked by numerous small spherical substances. Following the combined analysis with energy-dispersive X-ray spectrometer (EDS), the results

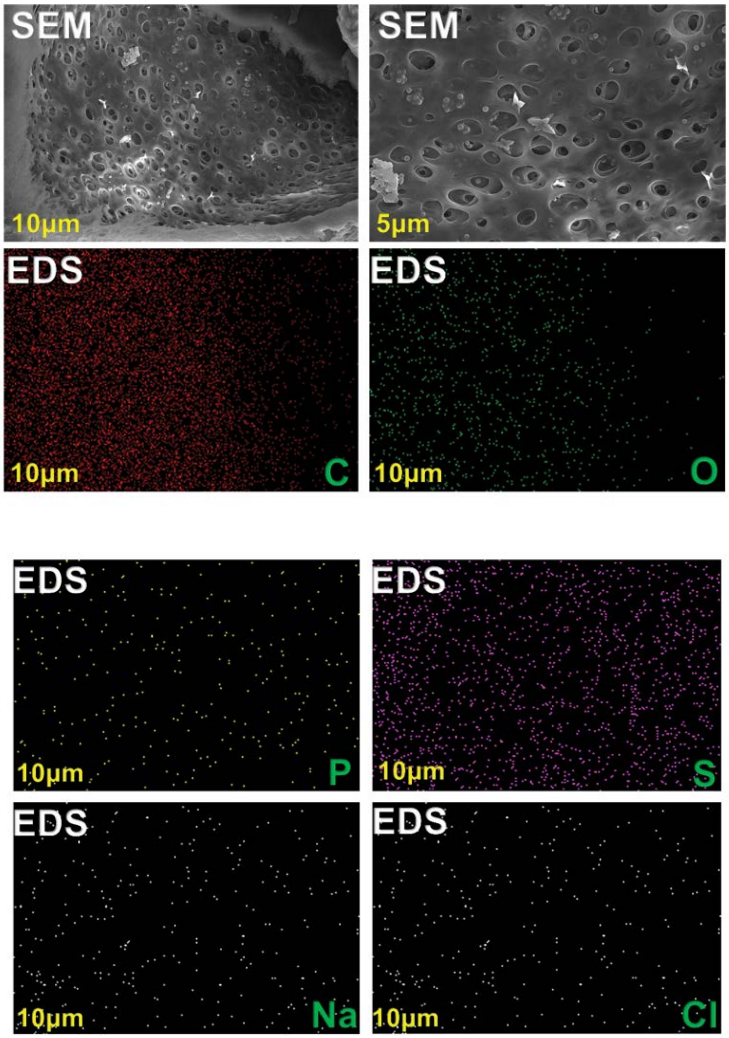


Fig. 7. SEM and EDS of polluted 150 Da membrane.

showed that C and O accounted for 97.09% of the elements in the EDS, followed by S, P, Cl, and Na. This indicates that a large amount of organic matter has occupied the contaminated membrane surface, and tiny P accumulated on the membrane surface. Relative positions of each element were analyzed qualitatively using EDS on the dry polluted membrane surface, where Na and Cl have overlapping positions in EDS. Therefore, for nanofiltration membranes that have been contaminated for a long time, acid washing should be used to remove surface organic matter and extend the use cycle of nanofiltration membranes for economic and energy savings.

## 4. Conclusion

A comprehensive study of the combined UF-NF separation system found that this composite process has a more significant potential for efficient phosphorus removal and sodium chloride retention and can make a breakthrough in the treatment of highly concentrated waste salt. It shows that the combined ultrafiltration–nanofiltration separation is feasible for phosphorus removal from glyphosate by-product waste salt solution.

- Compared with single-stage nanofiltration separation to remove total phosphorus in the waste salt solution, the combined UF-NF secondary membrane separation process has a better removal ability for total phosphorus. It is mainly reflected in alleviating the deposition of large molecular weight impurities on the surface of the nanofiltration and the fact that some of the total phosphorus has been retained by the UF membrane, which significantly extends the service life of the nanofiltration.
- The total phosphorus removal rate of the waste salt solution obtained by the secondary membrane separation was 96%. The sodium chloride removal rate was 46% at an initial pH of 10 and a concentration of 330 g/L, with a molecular weight cutoff of 5,000 Da retained by the ultrafiltration membrane and a lay pressure of 0.4 MPa. The nanofiltration kept a molecular weight cut-off of

150 Da and an applied pressure of 2.6 MPa. At 2.6 MPa, the NF membrane flux is 210 L/m²·h.

- Most of the larger molecules are removed and blocked in the stomata to affect the efficiency of the membrane seriously. For membrane cleaning, it is essential to focus not only on the cleaning of the membrane itself but also on the cleaning of the stomata on the membrane surface coating. The above research results show the practicality of the UF-NF secondary separation process in actual production and provide a reference for treating related industrial wastewater.

**Funding**

This work was supported by the National Key Research and Development Program (2019YFC1905800) from China.

**Acknowledgments**

Thanks to Hubei Xingfa Chemical Group Co., Ltd. for providing glyphosate by-product salt.

**Statements and declarations**

No competing financial interests exist.

**References**

[1] J. Clapp, Explaining growing glyphosate use: the political economy of herbicide-dependent agriculture, Global Environ. Change., 67 (2021) 102239.
[2] Z.Q. Liu, M.M. Lu, X.H. Zhang, F. Cheng, J.M. Xu, Y.P. Xue, L.Q. Jin, Y.S. Wang,Y.G. Zheng, Significant improvement of the nitrilase activity by semi-rational protein engineering and its application in the production of iminodiacetic acid, Int. J. Biol. Macromol., 116 (2018) 563–571.
[3] M. Xie, Z. Liu,Y. Xu, Removal of glyphosate in neutralization liquor from the glycine-dimethylphosphit process by nanofiltration, J. Hazard. Mater., 181 (2010) 975–980.
[4] B. Xing, H. Chen, X.J.E.T. Zhang, Efficient degradation of organic phosphorus in glyphosate wastewater by catalytic wet oxidation using modified activated carbon as a catalyst, Environ. Technol., 39 (2017) 749–758.
[5] V.E.C. da Silva, Y.S. Tadayozzi, F.F. Putti, F.A. Santos, J.C. Forti, Degradation of commercial glyphosate-based herbicide via advanced oxidative processes in aqueous media and phytotoxicity evaluation using maize seeds, Sci. Total Environ., 840 (2022), 156656, doi: 10.1016/j.scitotenv.2022.156656.
[6] Q.S. Wu, M. Jiang, W.J. Zhang, T. Jiang, M.F. Cui, B.J. Xi, Q.W. Han, Modified attapulgite for phosphorus removal from glyphosate by-product salt solution, Desal. Water Treat., 253 (2022) 100–112.
[7] H.M. Huang, P. Zhang, L.P. Yang, D.D. Zhang, G.J. Guo, J.H. Liu, A pilot-scale investigation on the recovery of zinc and phosphate from phosphating wastewater by step precipitation and crystallization, Chem. Eng. J., 317 (2017) 640–650.
[8] F. Sher, K. Hanif, S.Z. Iqbal, M. Imran, Implications of advanced wastewater treatment: electrocoagulation and electroflocculation of effluent discharged from a wastewater treatment plant, J. Water Process Eng., 33 (2020) 101101, doi: 10.1016/j.jwpe.2019.101101.
[9] A. Biswas, S.K. Patidar, Organics and phosphorus removal in circular flow corridor constructed wetland system, J. Water Process Eng., 49 (2022) 103015, doi: 10.1016/j.jwpe.2022.103015.
[10] Y. Wang, X. Yang, Y. Jiang, X. Dai, J. Dai, Y. Yan, M. Dong, L. Chen, Simultaneous removal of phosphorus and soluble organic pollutants by a novel organic/inorganic nanocomposite membrane via $Zr(OH)_4$ in-situ decoration, J. Taiwan Inst. Chem. Eng., 131 (2022) 104165, doi: 10.1016/j.jtice.2021.104165.
[11] W.-J. Xia, L.-X. Guo, L.-Q. Yu, Q. Zhang, J.-R. Xiong, X.-Y. Zhu, X.-C. Wang, B.-C. Huang, R.-C. Jin, Phosphorus removal from diluted wastewaters using a La/C nanocomposite-doped membrane with adsorption-filtration dual functions, Chem. Eng. J., 405 (2021) 126924, doi: 10.1016/j.cej.2020.126924.
[12] H.M. Azam, S.T. Alam, M. Hasan, D.D.S. Yameogo, A.D. Kannan, A. Rahman, M.J. Kwon, Phosphorous in the environment: characteristics with distribution and effects, removal mechanisms, treatment technologies, and factors affecting recovery as minerals in natural and engineered systems, Environ. Sci. Pollut. Res., 26 (2019) 20183–20207.
[13] H.E. Gray, T. Powell, S. Choi, D.S. Smith, W.J. Parker, Organic phosphorus removal using an integrated advanced oxidation-ultrafiltration process, Water Res., 182 (2020) 115968, doi: 10.1016/j.watres.2020.115968.
[14] N. Couto, P. Guedes, A.R. Ferreira, M.R. Teixeira, E.P. Mateus, A.B. Ribeiro, Electrodialytic process of nanofiltration concentrates – phosphorus recovery and microcystins removal, Electrochim. Acta, 181 (2015) 200–207.
[15] K. Arola, M. Mänttäri, M. Kallioinen, Two-stage nanofiltration for purification of membrane bioreactor treated municipal wastewater – minimization of concentrate volume and simultaneous recovery of phosphorus, Sep. Purif. Technol., 256 (2021) 117255, doi: 10.1016/j.seppur.2020.117255.
[16] Y.-J. Shen, L.-F. Fang, Y. Yan, J.-J. Yuan, Z.-Q. Gan, X.-Z. Wei, B.-K. Zhu, Metal-organic composite membrane with sub-2 nm pores fabricated via interfacial coordination, J. Membr. Sci., 587 (2019) 117146, doi: 10.1016/j.memsci.2019.05.070.
[17] Y.K. Chai, H.C. Lam, C.H. Koo, W.J. Lau, S.O. Lai, A.F. Ismail, Performance evaluation of polyamide nanofiltration membranes for phosphorus removal process and their stability against strong acid/alkali solution, Chin. J. Chem. Eng., 27 (2019) 1789–1797.
[18] S. Zhao, Y. Yao, C. Ba, W. Zheng, J. Economy, P. Wang, Enhancing the performance of polyethylenimine modified nanofiltration membrane by coating a layer of sulfonated poly(ether ether ketone) for removing sulfamerazine, J. Membr. Sci., 492 (2015) 620–629.
[19] L.F. Fang, M.Y. Zhou, L. Cheng, B.K. Zhu, H. Matsuyama, S.F. Zhao, Positively charged nanofiltration membrane based on cross-linked polyvinyl chloride copolymer, J. Membr. Sci., 572 (2019) 28–37.
[20] Y.J. Shen, Q.R. Kong, L.F. Fang, Z.L. Qiu, B.K. Zhu, Construction of covalently-bonded tannic acid/polyhedral oligomeric silsesquioxanes nanochannel layer for antibiotics/salt separation, J. Membr. Sci., 623 (2021) 119044, doi: 10.1016/j.memsci.2020.119044.
[21] J. Jang, Y. Kang, K. Jang, S. Kim, S.-S. Chee, I.S. Kim, $Ti_3C_2T_X$-Ethylenediamine nanofiltration membrane for high rejection of heavy metals, Chem. Eng. J., 437 (2022) 135297, doi: 10.1016/j.cej.2022.135297.
[22] J. Yu, Y. Wang, Y. He, Y. Gao, R. Hou, J. Ma, L. Zhang, X. Guo, L. Chen, Calcium ion-sodium alginate double cross-linked graphene oxide nanofiltration membrane with enhanced stability for efficient separation of dyes, Sep. Purif. Technol., 276 (2021) 119348, doi: 10.1016/j.seppur.2021.119348.
[23] H.-F. Xiao, C.-H. Chu, W.-T. Xu, B.-Z. Chen, X.-H. Ju, W. Xing, S.-P. Sun, Amphibian-inspired amino acid ionic liquid functionalized nanofiltration membranes with high water permeability and ion selectivity for pigment wastewater treatment, J. Membr. Sci., 586 (2019) 44–52.
[24] S. Castaño Osorio, P.M. Biesheuvel, J.E. Dykstra, E. Virga, Nanofiltration of complex mixtures: the effect of the adsorption of divalent ions on membrane retention, Desalination, 527 (2022) 115552, doi: 10.1016/j.desal.2022.115552.
[25] Y. Du, Y. Lv, W.Z. Qiu, J. Wu, Z.K. Xu, Nanofiltration membranes with narrowed pore size distribution via pore wall modification, Chem. Commun., 52 (2016) 8589–8592.
[26] M. Park, J. Park, E. Lee, J. Khim, J. Cho, Application of nanofiltration pretreatment to remove divalent ions for

economical seawater reverse osmosis desalination, Desal. Water Treat., 57 (2016) 20661–20670.
[27] G. Bargeman, M. Steensma, A. Ten Kate, J.B. Westerink, R.L.M. Demmer, H. Bakkenes, C.F.H. Manuhutu, Nanofiltration as energy-efficient solution for sulfate waste in vacuum salt production, Desalination, 245 (2009) 460–468.
[28] Z. Abdorrezaee, A. Raisi, A hybrid ultrafiltration/nanofiltration/pervaporation membrane process for intensifying the refining of crude canola oil and solvent recovery, Chem. Eng. Process. Process Intensif., 169 (2021) 108598, doi: 10.1016/j.cep.2021.108598.
[29] A. Vaysizadeh, A.A. Zinatizadeh, S. Zinadini, Fouling mitigation and enhanced dye rejection in UF and NF membranes via layer-by-layer (LBL) assembly and altering PVP percentage as pore former, Environ. Technol. Innovation, 23 (2021) 101698, doi: 10.1016/j.eti.2021.101698.
[30] M.F. Tay, C. Liu, E.R. Cornelissen, B. Wu, T.H. Chong, The feasibility of nanofiltration membrane bioreactor (NF-MBR)+reverse osmosis (RO) process for water reclamation: comparison with ultrafiltration membrane bioreactor (UF-MBR)+RO process, Water Res., 129 (2018) 180–189.
[31] Y. Chung, D. Park, H. Kim, S.E. Nam, S. Kang, Novel method for the facile control of molecular weight cut-off (MWCO) of ceramic membranes, Water Res., 215 (2022) 118268.
[32] W.P.C. Lee, S.K. Mah, C.P. Leo, T.Y. Wu, S.P. Chai, Performance studies of phosphorus removal using cross-flow nanofiltration, Desal. Water Treat., 52 (2014) 5974–5982.
[33] J.L. Wang, X.B. Tang, Y.F. Xu, X.X. Cheng, G.B. Li, H. Liang, Hybrid UF/NF process treating secondary effluent of wastewater treatment plants for potable water reuse: adsorption vs. coagulation for removal improvements and membrane fouling alleviation, Environ. Res., 188 (2020) 109833, doi: 10.1016/j.envres.2020.109833.
[34] G.D. Fan, Z.S. Li, Z.S. Yan, Z.Q. Wei, Y.G. Xiao, S.B. Chen, H.D. Shangguan, H. Lin, H.Q. Chang, Operating parameters optimization of combined UF/NF dual-membrane process for brackish water treatment and its application performance in municipal drinking water treatment plant, J. Water Process Eng., 38 (2020) 101547, doi: 10.1016/j.jwpe.2020.101547.
[35] M.C.S. Amaral, L.B. Grossi, R.L. Ramos, B.C. Ricci, L.H. Andrade, Integrated UF-NF-RO route for gold mining effluent treatment: from bench-scale to pilot-scale, Desalination, 440 (2018) 111–121.
[36] X. Tang, J.C. Zhang, Z.J. Jin, J.Y. Xiong, L.M. Lin, Y.X. Yu, S.B. Han, Experimental investigation of thermal maturation on shale reservoir properties from hydrous pyrolysis of Chang 7 shale, Ordos Basin, Mar. Pet. Geol., 64 (2015) 165–172.
[37] Reverse Osmosis: Membrane Technology, Water Chemistry and Industrial Applications, Van Nostrand Reinhold, New York, 1993.
[38] Y.H. Li, S.H. Wang, H.Y. Li, G.D. Kang, Y. Sun, H.J. Yu, Y. Jin, Y.M. Cao, Preparation of highly selective nanofiltration membranes by moderately increasing pore size and optimizing microstructure of polyamide layer, J. Membr. Sci., 643 (2022) 120056, doi: 10.1016/j.memsci.2021.120056.
[39] P. Sarkar, S. Modak, S. Karan, Ultraselective and highly permeable polyamide nanofilms for ionic and molecular nanofiltration, Adv. Funct. Mater., 31 (2021) 2007054, doi: 10.1002/adfm.202007054.
[40] F.C. Kramer, R. Shang, L.C. Rietveld, S.J.G. Heijman, Influence of pH, multivalent counter ions, and membrane fouling on phosphate retention during ceramic nanofiltration, Sep. Purif. Technol., 227 (2019) 115675, doi: 10.1016/j.seppur.2019.115675.
[41] W.-H. Yu, Z.-Q. Gan, J.-R. Wang, Y. Zhao, J. Han, L.-F. Fang, X.-Z. Wei, Z.-L. Qiu, B.-K. Zhu, A novel negatively charged nanofiltration membrane with improved and stable rejection of Cr(VI) and phosphate under different pH conditions, J. Membr. Sci., 639 (2021) 119756, doi: 10.1016/j.memsci.2021.119756.
[42] G. Yang, W.H. Xing, N.P. Xu, Concentration and diafiltration of aqueous fluorescent whitener solution by nanofiltration, Desalination, 150 (2002) 155–164.
[43] M. Xie, Y.H. Xu, Partial desalination and concentration of glyphosate liquor by nanofiltration, J. Hazard. Mater., 186 (2011) 960–964.
[44] W. Gao, H. Liang, J. Ma, M. Han, Z.L. Chen, Z.S. Han, G.B. Li, Membrane fouling control in ultrafiltration technology for drinking water production: a review, Desalination, 272 (2011) 1–8.
[45] G. Mustafa, K. Wyns, A. Buekenhoudt, V. Meynen, New insights into the fouling mechanism of dissolved organic matter applying nanofiltration membranes with a variety of surface chemistries, Water Res., 93 (2016) 195–204.